Developing achromatic coronagraphic optics for LMIRCam and the LBT

Matthew A. Kenworthy[a,b], Philip M. Hinz[a], Johanan L. Codona[a], John C. Wilson[c], Michael F. Skrutskie[c], Elliott Solheid[a]

[a]Leiden Observatory, Leiden University, P.O. Box 9513, 2300 RA Leiden, The Netherlands;
[b]Steward Observatory, 933 N. Cherry Avenue, Tucson, AZ 85721, USA;
[c]University of Virginia, 530 McCormick Rd, Charlottesville, VA, 22904, USA

ABSTRACT

The Apodizing Phase Plate (APP) is a simple optic that provides coronagraphic suppression of diffraction without the need for any focal plane occulters. We present the design of a broadband APP (the BAPP) for LMIRCam that is optimised for the direct imaging of cool extrasolar giant planets around nearby stars at thermal infrared wavelengths. These optics have a high throughput and require no precision alignment. We cover earlier results using a chromatic APP, the basic principle and manufacture of the optic.

Keywords: coronagraph, LMIRcam, thermal imaging, extrasolar planets, apodizing, apodizing phase plate

1. INTRODUCTION

We are designing and testing a Broadband Apodizing Phase Plate (BAPP), using the same principles in traditional achromatic lens doublets, to form an ideal APP at two or three defined wavelengths. The benefits of the BAPP are a much broader null over a wider wavelength regime and less stringent manufacturing tolerances. The BAPP will enable the detection and characterization of extrasolar giant planets as old as 2 Gyr and down to the M_{jup} regime in to a few AU.

Of all the capabilities offered by the tremendous collecting area of the Large Binocular Telescope (LBT) among the most attractive are the 22.8-meter baseline and the low thermal background for mid-infrared observations offered by carrying this two-mirror interferometer on a single platform. The combined light of the two primary mirrors yields a true diffraction limited Fizeau image plane limited only by the isoplanatic angle. As opposed to traditional interferometers the LBT optical path is fully cryogenic once past the telescope primaries, adaptive secondaries, and tertiary mirrors. LMIRcam[1](L/M-band Infrared Camera) fills an important wavelength gap in the LBT's first generation instrumentation by incorporating a mid-infrared imager operating primarily in the L ($3.6\mu m$) and M ($4.8\mu m$) infrared atmospheric windows. It is located inside the $10\mu m$ nulling/imaging system at the LBT's combined focus (see Figure 1).

2. THE DIRECT IMAGING OF EXTRASOLAR GIANT PLANETS

From a geometric consideration of the solid angle subtended by Jupiter as seen from the Sun, little more than 10^{-9} of the Sun's light is reflected from the planet's disk, and even at the relatively close distance of $5pc$, an extrasolar Jupiter would be just one arcsecond away from the parent star. The planet's signal is buried in the noise of the diffracted and scattered light of the primary star. Theoretical modeling of the spectra of extrasolar planets reveals that Jupiter and other giant planets glow in the thermal infrared due to the leftover heat from their formation.[2]Jupiter has a thermal radiation spectrum that peaks in the mid infrared,[3] resulting in a planet-to-star flux ratio 100 to 1000 times larger than that in the visible.

The theoretical spectral energy distributions (SEDs) of gas giant planets ($< 13\ M_{jup}; T_{eff} < 1300\ K$ for ages > 100 Myr) show a strong peak[2] around $\sim 5\mu m$(see Figure 2). While direct imaging surveys for substellar companions to nearby stars have concentrated on the H band, theory predicts that the $3-5\mu m$ fluxes for planets

Send correspondence to M.A.K. E-mail: kenworthy@strw.leidenuniv.nl, Telephone: +31 (0)71 527 8455

Optical and Infrared Interferometry II, edited by William C. Danchi, Françoise Delplancke, Jayadev K. Rajagopal,
Proc. of SPIE Vol. 7734, 77342P · © 2010 SPIE · CCC code: 0277-786X/10/$18 · doi: 10.1117/12.856819

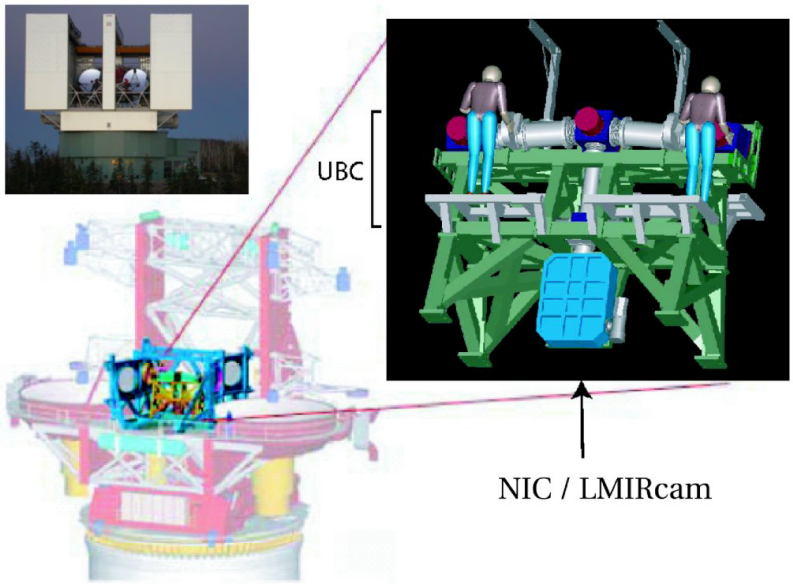

Figure 1. Location of LMIRcam within the LBT structure.

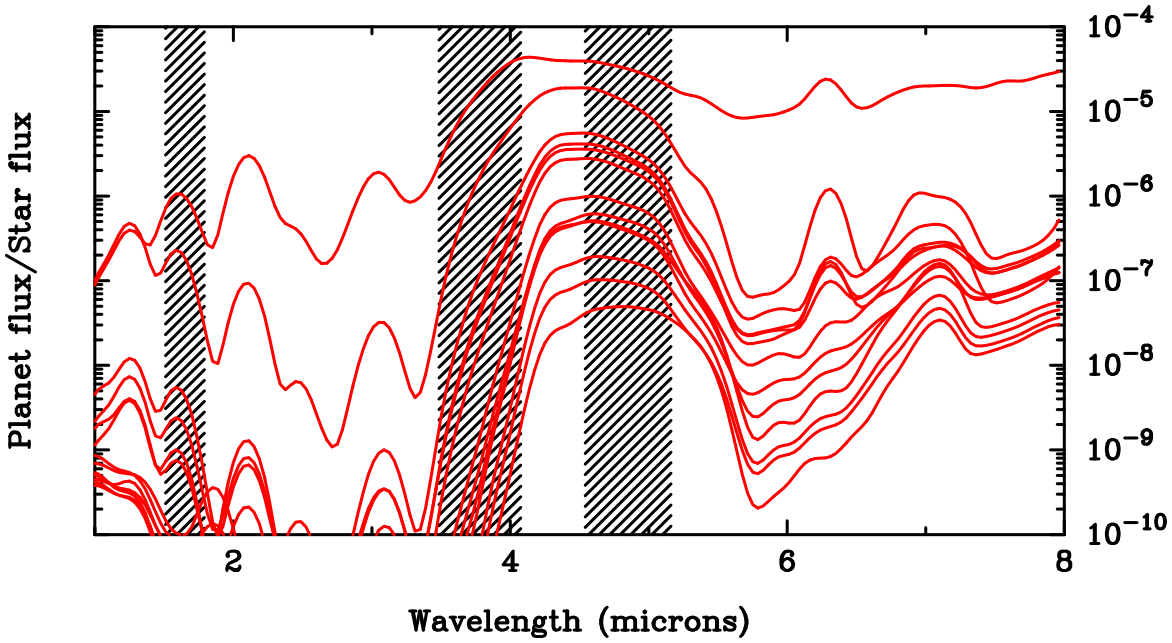

Figure 2. Theoretical contrast spectra of the 12 exoplanet candidates with the best contrast for direct imaging.[4] H, L' and M bands are indicated in the shaded regions centered on 1.65, 3.78 and 4.85μm respectively. All spectra show the broad spectral feature at M band discussed in the text, from the massive EGP at the topmost curve (HD 39091b, $M_p \sin i = 10.3 M_{jup}$), to the lowest mass planet at the bottom (47 UMa c, $M_p \sin i = 0.76 M_{jup}$). Spectra are smoothed with a Gaussian filter of width 0.2μm.

should be much brighter than at $1-2\mu m$ for ages of > 0.1 Gyr (e.g. a $10\,M_{jup}$ object at 0.5 Gyr has colors of $J-M \simeq 4$, $K-M \simeq 6$, $L-M \simeq 1$).[5]

The direct imaging of bona-fide exoplanets has begun in earnest, with detections of three planets around HR 8799,[6] a $< 3M_{jup}$ planet in orbit around Fomalhaut,[7] and most recently, the confirmation of a $7-11M_{jup}$ planet around β Pictoris[8] and a confirmation of a $7-12M_{jup}$ planetary mass companion to a solar analog[9,10] with a separation of 330 AU provides new challenges to current theories of planet formation. The "hot start" giant planet models[5,11] have led several direct imaging groups to search for extrasolar planets in the H and K band infrared windows, where the models indicate a significant planet flux above that expected from a simple blackbody model and the sky background is low enough for ground based telescopes at good astronomical sites. Two of these groups[12,13] concluded their surveys in 2007 with no confirmed planetary detections. Other groups have concentrated at longer wavelengths such as L' and M band, notably an L' band survey by[14] reporting no detections around a selection of late type stars, and[15] carried out an L' band survey around 50 nearby solar type stars using the Clio thermal infrared camera at the MMTO 6.5m telescope in Arizona.

They are limited at small angular separations **not** by the sky background, but by the presence of time-varying systematic noise ("super-speckles") modulated by the diffracted light from the central star. It is important to note that the super-speckle noise does not average out as sqrt(t)[16,17] and that for bright targets diffraction suppression methods represent the only method for direct exoplanet detection at small angular separations. It is interesting to note that although the SDI methods[13,18,19] help mitigate the super-speckle noise, they are still affected by chromatic effects, small bandwidth, and non-common path errors in the optics of the instrument. Longer integrations do not help resolve planets that are buried within the diffraction pattern of the primary star.

To optimise the detection of an exoplanet, we need to:

- **Maximise the flux from the exoplanet:** This means that we require as broad a spectral bandwidth as possible without increasing the sky background by exceeding the edges of the atmospheric transmission windows, *and* selecting a wavelength window where the contrast between planet and star is optimal.
- **Minimise the scattered light from the host star:** Using a coronagraph to suppress the host star light whilst maximising the exoplanet flux throughput and the minimization of quasi-static speckles due to non-common path aberrations.
- **Get as close to the star as possible:** Several high contrast coronagraph designs use a focal plane mask to obstruct light from the host star, but these also attenuate flux from the exoplanet - these coronagraphs have a trade-off between host star suppression and inner working angle (IWA) limited to several diffraction widths $(3-5\lambda/D)$ of the telescope system.

In the next section, we present a coronagraphic optic that can fulfill all of these requirements in an efficient way - the apodizing phase plate.

3. INITIAL ON-SKY TESTS WITH AN APP AT THE MMTO

The 6.5m MMTO telescope is the first realization of a large aperture telescope coupled with a deformable secondary mirror that delivers an AO corrected $f/15$ beam. Currently the system achieves typical Strehl ratios of 85% at M band.[20] Measurements taken with the BLINC/MIRAC mid-IR camera recorded the first ever high Strehl AO images taken at $10\mu m$, with a Strehl ratio of order 96%.

At longer wavelengths ($> 2.5\mu m$) the MMT AO system is uniquely sensitive because of the lower background light it emits at infrared wavelengths compared to conventional AO systems. This is because it uses a deformable secondary mirror for wavefront correction[21] which has the advantage of eliminating approximately 8 warm, dusty, optical surfaces from the typical AO system design.[22] The elimination of these extra optical surfaces (that are required for conventional large telescope AO systems e.g., Keck, VLT, etc.) allows the MMT AO to have much lower scattered light and lower thermal emissivity, whilst increasing the system throughput. We have determined that the 6.5 m MMT AO system in conventional imaging mode is as efficient as the 10 m Keck AO system at H ($1.6\mu m$) and 2.28 times as efficient at N ($10.5\mu m$) despite having a smaller primary mirror (for more on the

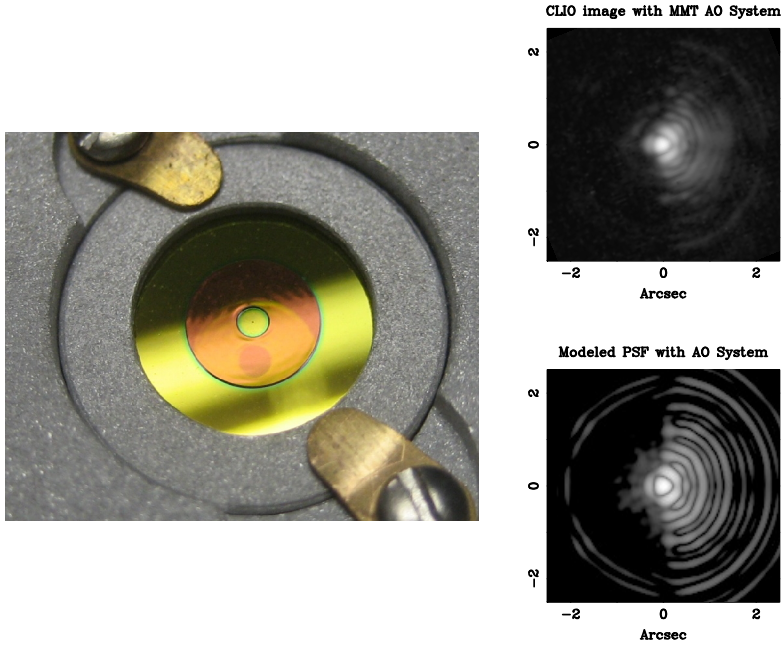

Figure 3. The CLIO/MMTO Apodizing Phase Plate and its effect on the telescope PSF. The bright yellow surface is a gold mask that matches the size of the telescope pupil, and the darker region forming an annulus shows the transmitting area of the APP that induces the phase apodization. The optic is a diamond turned Zinc Selenide transmissive substrate. On the right hand side, on-sky data from the APP at M band and below that, a simulated PSF at 85% Strehl as comparison.

MMT AO system see[21,23,24]). The emissivity of the MMT system has been measured to be approximately 7% in thermal infrared observations (Hinz, priv. commun.). This is already much improved over the 20% emissivity expected of conventional AO systems. Where telescope background is the dominant source of background photons (as it is for the most transparent portions of the L band and portions of the M band atmospheric window), a reduction in emissivity corresponds to a direct reduction in exposure time to reach a particular sensitivity.

The Clio camera[25,26] consists of a $5\mu m$ camera that is optimised to work with diffraction limited images in H, L' and M bands. An $f/20$ imaging mode is optimised to work in the high background regime of L' and M bands with Nyquist sampling at L' band (0.048"/pixel) and a field of view of 15" by 12". It contains a high-well-depth, fast read-out InSb detector, and was designed specifically to image wide-separation giant planets around nearby stars. The combination of Clio at the 6.5m MMTO provides us with a testbed for novel coronagraphic optics such as the APP.

Coronagraphs are employed to reduce the light scattered in the telescope optics from diffraction, but at a cost of throughput and angular resolution.[27] provide a comparison of many types of high contrast coronagraphs. At Steward Observatory, we have implemented a new type of coronagraphic optic called the **Apodizing Phase Plate (APP)**, based on the theory of Phase Apodization Coronagraphy,[28,29] which suppresses diffraction from a central target star over 180° in a "D" shaped region surrounding the central star **at very little cost in throughput and angular resolution.** By suppressing the stellar diffraction, we also suppress the quasi-static super speckles which are modulated by the diffraction signal, whilst letting the flux from the EGP through. By rotating the instrument by 180 degrees, we can search all the way around the target star with the enhanced sensitivity as demonstrated in on-sky observations.[20] A comparison between direct imaging carried out[30] and APP data on Vega is shown in Figure 3. Note that *even without* speckle supression techniques such as PSI[31] we are reaching a contrast of 11 magnitudes at $3\lambda/D$ (0.5 arcsec) with this chromatic APP.

Because the optic only modulates the *phase* of the incoming wavefront, there is no requirement for a focal plane coronagraphic disk to obscure the host star, and so all objects in the field of view have exactly the same APP PSF - **the APP requires no special alignment with the host star**. Many other coronagraph designs

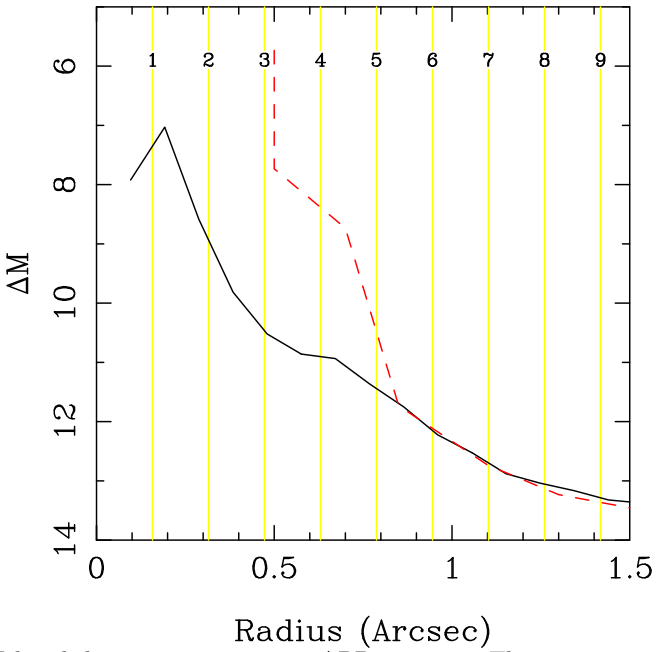

Figure 4. A comparison of M band direct imaging versus APP imaging. The curves represent the 5σ source detection limit in 1 hour over an azimuthally averaged segment of 150 degrees. The red dashed line is direct imaging data.[30] The APP outperforms direct imaging at distances smaller than 0.8 arcseconds ($5\lambda/D$). The sensitivity loss at < 1 arcsecond is due to the presence of "quasi-static speckles" and not manufacturing errors in the APP.

that use a focal plane mask or focal plane apodization require high pointing and tracking stability for optimal performance.[27] The APP does not require such a specific location on the array, and so we can beam switch with no overhead whatsoever for focal plane mask alignment.

In addition, there is no amplitude apodization - all of the flux of the pupil is transmitted through the APP, only the phase is modified. Since we are using light from the core of the PSF to suppress diffraction over one half of the PSF, there is a reduction in the core intensity of all objects in the field of view of the camera, including the planet and host star. The degree of core flux lost is a trade-off between level of suppression, the smallest inner working angle that the suppression can go to, and the core flux.[32] We chose an (APP/Direct Imaging) core flux ratio of 70% (see Figure 3). The integration required to get complete coverage around a host star and reach the same signal to noise as direct imaging is 4 times longer, but this is more than compensated for by the **additional sensitivity at small IWAs which are otherwise inaccessible without a coronagraph.**

4. THE BROADBAND APP DESIGN

In the original APP design,[20] variations in the thickness of a Zinc Selenide substrate introduces optical path differences that correspond to variations in phase across the telescope pupil (see Figure 3). The variation in phase, $\Delta\phi$, is related to variations in the thickness of the substrate Δx by the refractive index n of the transmitting material: $\Delta\phi = (2\pi/\lambda).\Delta x.(n-1)$, which is an inherently chromatic process.

By choosing two different IR transmitting materials with similiar refractive indicies, a large optical path difference introduced by one plate can be almost completely removed by another plate with a suitably scaled opposing phase pattern generated in the other material - the concept is shown in Figure 5. In the right-hand panel of Figure 5, the graph shows the effective phase shift of a BAPP as a function of wavelength. A completely ideal, achromatic APP is represented by the horizontal blue line at a relative normalised scale height of unity. With the two infra-red transmitting glasses of Zinc Selenide and Zinc Sulphide, we can achieve an achromatic null within 2% from $3.5 - 8\mu m$ with a single assembled BAPP.

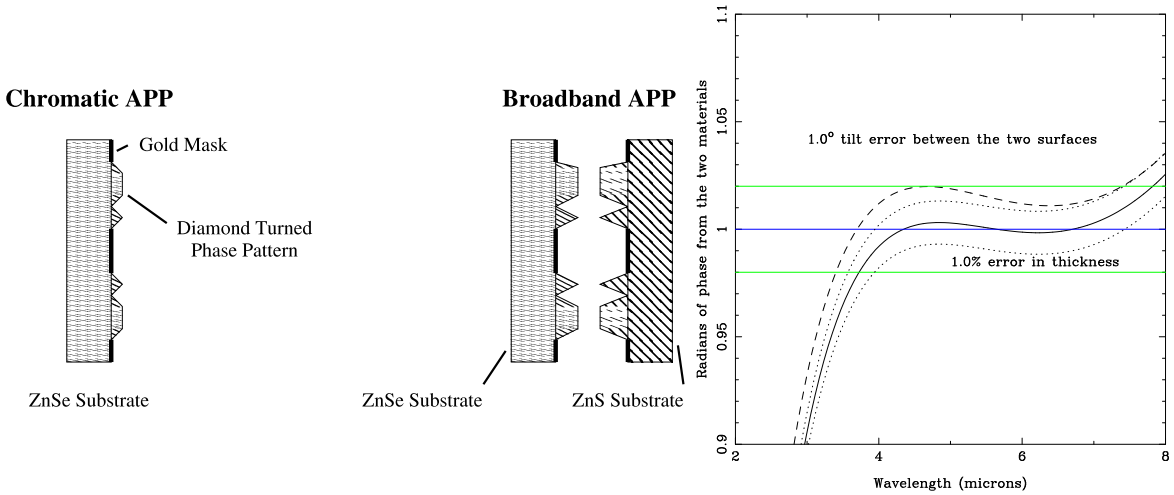

Figure 5. Broadband APP principle. The basic APP has a diamond turned phase pattern on one surface of a ZnSe substrate. In the Broadband APP, the same pattern is inscribed into two different substrates, with the two plates facing each other. The scale height of the phase pattern is increased by a factor of 30 as Zinc Sulphide and Zinc Selenide have similar indices of refraction.

We also carried out basic tolerancing of this design by investigating the effects of tilting the two plates with respect to each other by one degree, and a relative machining systematic error of 1%, represented by the dashed line and dotted lines respectively in Figure 5. The BAPP does not deviate significantly beyond the 2% tolerance, demonstrating that the BAPP can be assembled and mechanically aligned with no fundamentally challenging machining tolerances.

Building a BAPP has several advantages, including (i) Broadband suppression across both L' and M bands with the same optic, so any quasistatic offsets between L' and M band will be similiar in magnitude and location, and (ii) A technology demonstrator of BAPP at shorter wavelengths (such as H and K band) using currently proven diamond turning technology.

5. THERMAL IMAGING AT THE LBT WITH LMIRCAM

The Large Binocular Telescope consists of two 8.4-m primaries separated by 14.4-m on a common telescope mount. Deformable adaptive secondary mirrors (ASMs) provide correction for atmospheric turbulence. Tertiary mirrors fold the light to an instrument platform between the mirrors, where the $f/15$ beams form two image planes. The LBT Interferometer (LBTI) occupies the central instrument platform of the telescope. Telescope construction is complete with first light at prime focus with each telescope achieved in 2005 and 2006 respectively. Each ASM consists of a thin zerodur deformable shell and matching rigid reference body fabricated by the Mirror Lab at Steward Observatory, as well as 670 electromagnetic force actuators and associated position sensors, fabricated by Arcetri Observatory in association with Microgate.[33,34] The two LBT systems are being fabricated by the same collaboration that developed the prototype adaptive secondary for the MMT.

The Large Binocular Telescope Interferometer (LBTI) takes advantage of this unique mirror configuration. The instrument is both a general purpose high resolution imager, and a precision nulling interferometer capable of extrasolar zodiacal dust and giant planet detection. The first-stage of the LBTI is a general purpose re-imager, called the Universal Beam-Combiner (UBC) which re-images the individual focal planes of the telescopes to a common image plane, while preserving the sine condition of the interferometer. This configuration allows interference over a field-of-view limited only by the isoplanatic patch of the adaptive optics correction.

The L/M-band Infrared Camera (LMIRcam) resides inside the $10\mu m$ nulling/imaging system now under construction for the LBT's combined focus. The adaptive secondary mirrors needed to enable coherent combination of the two mirror's beams at high strehl are part of the LBT's baseline implementation, the first of the two adaptive secondary mirrors achieved closed loop operation in Spring 2010, with the second mirror planned

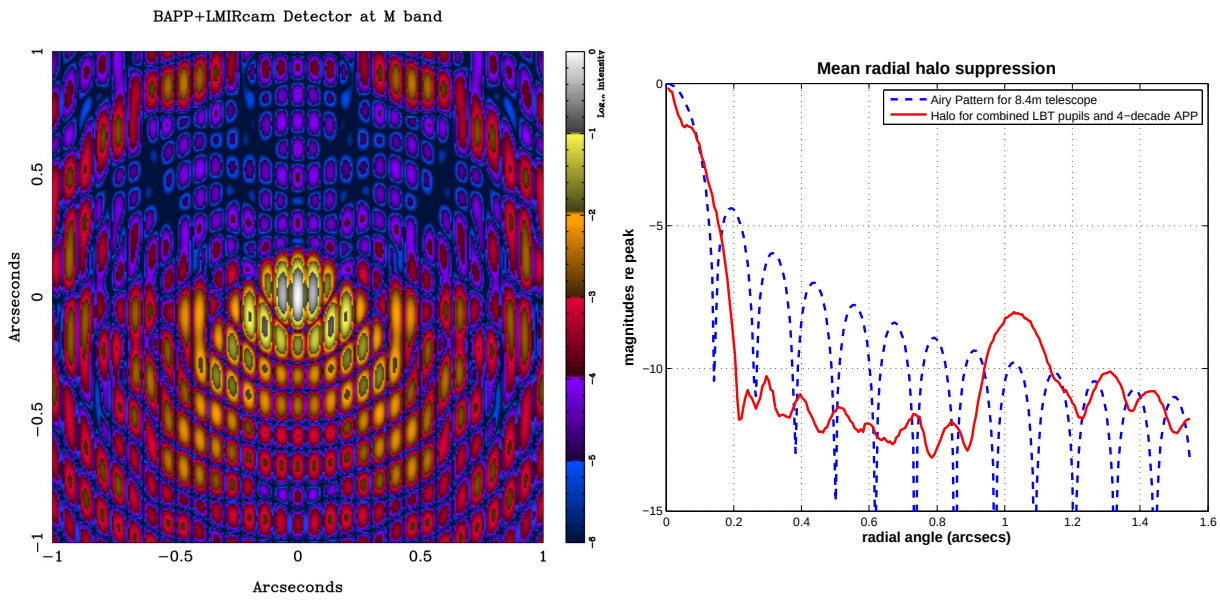

Figure 6. The BAPP PSF for LMIRcam with a logarithmic scale normalised to the central fringe peak. The left-hand image shows the PSF for LMIRcam at M band, and the right hand image shows the azimuthally averaged PSF for both the direct imaging PSF (dashed blue line) and and the BAPP PSF (solid red line). The BAPP PSF shows a diffraction suppression of 10 magnitudes at 0.3 arcseconds.

for 2011. NASA is supporting the development and construction of the LBT's cryogenic beam combiner (the "Universal Beam Combiner" or UBC) as well as the fabrication of the $10\mu m$ nulling camera, NIC, that will also house LMIRcam.

6. THE LBT BAPP

The LBT BAPP consists of two identical BAPP phase patterns inscribed onto optics within a single mount, matched to the twin pupils of the LBT. We have found that the presence of the secondary and tertiary mirror support structures do not significantly contribute to our theoretical BAPP PSF, which is confirmed by our practical experience at the MMT. The two APPs are oriented so that the dark D's point in the same direction, and the piston phase between the two telescopes is actively removed by the beam combiner system, forming a PSF composed of a single 8.4m telescope, modulated by the Young's fringes generated by the two telescope baseline of 22.8m (see Figure 6). The purpose of forming the coherent three-lobed PSF is *not* for additional spatial resolution on the sky, but for the enhancement in sensitivity the exoplanet PSF will have - the planet signal is dominated by noise from the sky background, so by performing photometry over the bright central narrow fringe instead of the 8.4m telescope Airy disk, we gain a factor of 2 in sensitivity at the LBT.

Our baseline design has a 70% core flux transmission and an IWA of $1.8\lambda/D$ (0.212 arcsec at $4.8\mu m$) with a contrast of 10 magnitudes. With the BAPP in place, we require 4 hours of on-sky time to reach the same sensitivity limits as for direct imaging - 2 hours for one sky orientation, and another 2 hours for the 180 degree orientation. In practice, we will have an additional BAPP that will be present in the filter wheel and rotated into place on subsequent nights to achieve full host star coverage.

7. SENSITIVITY LIMITS WITH LMIRCAM AND BAPP

The clean thermal path and cryogenically cooled beam combiner, together with the optically clean layout of LMIRcam leads to a point source sensitivity flux limit in one hour of integration (5σ) of 2μJy at $3.6\mu m$ and 20μJy at $4.8\mu m$ corresponding to Vega magnitudes of 20.5 and 17.3, comparable to space based observatories.[1] With the BAPP throughput of 70%, this changes to an L and M band magnitudes of 19.7 and 16.5 respectively.

With an M band magnitude limit of 16.5, we will be able to carry out a comprehensive survey of all older stars within $10pc$ for Jupiters with $T_{eff} > 270K$ (typically$< 1M_{jup}$ to several M_{jup}). For younger stars in local associations out to 50 pc we will be sensitive to planets $1M_{jup}$ and below. These observations will directly test giant planet formation and evolution theories.[35,36]

8. IMPLEMENTATION SCHEDULE AND OPERATING CONFIGURATIONS

The success of the LBT AO system in May 2010 has led us to develop an implementation schedule that allows science using a single aperture during late 2010, before the second AO system is installed and operational in 2012 - the two apertures for the LBT are referred to as SX and DX respectively.

The BAPP cannot be rotated with respect to the telescope mirror baseline, and so to gain full sky coverage around a target star we need two BAPPs per telescope aperture. For clarification, we label each BAPP using this terminology: SX_0 and SX_{180} represent two separate BAPP which are installed in the LMIRcam pupil wheel, and their orientations are such that their PSFs on the sky have their dark sectors complementing each other (see top of Figure 7). An observation one night with SX_0 is followed the next night with observations using SX_{180} to give a complete 360 degree coverage around a target star using the SX 8.4m aperture.

There are two characteristic modes of observation with the LBT BAPP:

- **SEARCH** - Here we use the LBT as two separate 8.4m telescopes to provide 360 degree coverage around a single target star. This mode is used for surveys, where broadband detection of extrasolar planets is required.
- **CHARACTERIZATION** - Here we combine the two 8.4m apertures to form the full 22m baseline BAPP PSF. This mode is used to obtain spectra of known exoplanets. The combined 22m baseline PSF increases the signal to noise of the measured spectrum when used with a grism.

These modes are illustrated in the cartoon in Figure 7. In all, we require three wheel positions to hold all the combinations of BAPPs to cover both observing modes in full LBT operation.

Table 1. Table of configurations of LBT BAPP observing in single aperture and double aperture modes.

	SINGLE APERTURE (2010)	DOUBLE APERTURE (2012)
SEARCH	BLANK, SX_0 BLANK, SX_{180}	SX_0, DX_{180}
CHARACTERIZATION	Same as above	SX_0, DX_0 SX_{180}, DX_{180}
Pupil Wheel Posistions	2	3

9. CONCLUSIONS

We are fabricating coronagraphic optics for the LBT LMIRcam that will lead to the detection and characterization of directly imaged extrasolar planets around nearby stars. The combination of the coronagraphic optics with the enhanced sensitivity and low background at thermal wavelengths will enable a new parameter space for exoplanet imaging and other high contrast science drivers at the LBT, and complement the shorter wavelength exoplanet searches of the SPHERE and the GPI instruments.

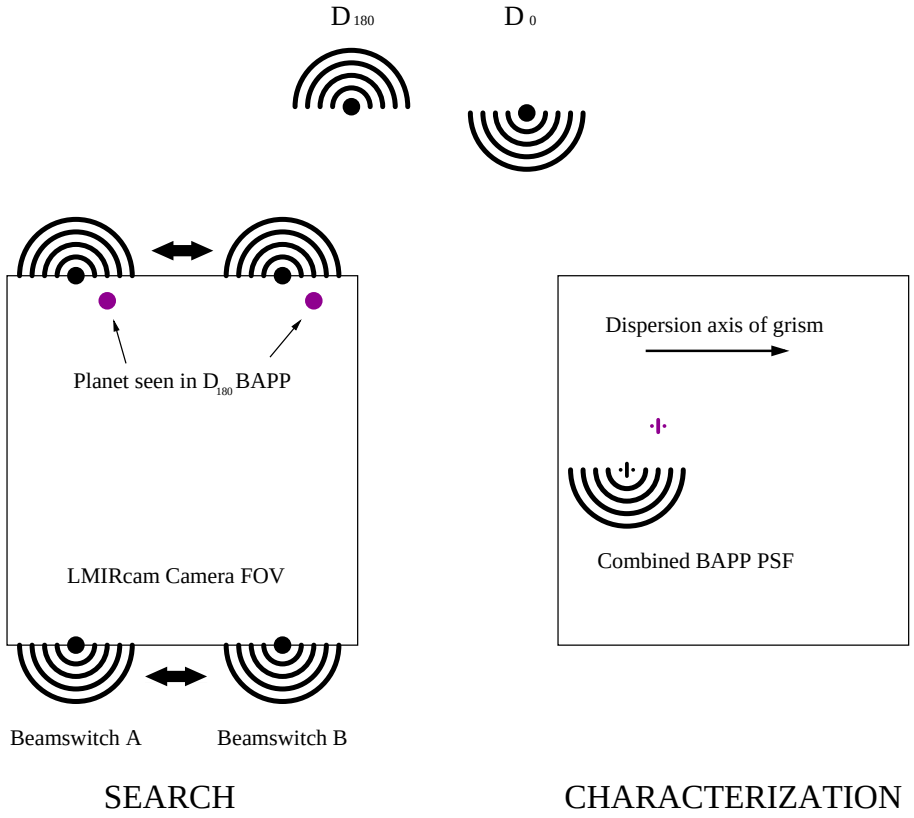

Figure 7. Orientation of the BAPP for LBT observing. The two observing modes are shown on the left and right of the figure. The characterization mode does not show the beamswitched image or the dispersed planet spectrum for clarity.

REFERENCES

[1] Wilson, J. C., Hinz, P. M., Skrutskie, M. F., Jones, T., Solheid, E., Leisenring, J., Garnavich, P., Kenworthy, M., Nelson, M. J., and Woodward, C. E., "LMIRcam: an L/M-band imager for the LBT combined focus," in [*Society of Photo-Optical Instrumentation Engineers (SPIE) Conference Series*], *Presented at the Society of Photo-Optical Instrumentation Engineers (SPIE) Conference* **7013** (July 2008).

[2] Burrows, A., Marley, M., Hubbard, W. B., Lunine, J. I., Guillot, T., Saumon, D., Freedman, R., Sudarsky, D., and Sharp, C., "A Nongray Theory of Extrasolar Giant Planets and Brown Dwarfs," *ApJ* **491**, 856–+ (Dec. 1997).

[3] Gillett, F. C., Low, F. J., and Stein, W. A., "The 2.8-14-MICRON Spectrum of Jupiter," *ApJ* **157**, 925–+ (Aug. 1969).

[4] Burrows, A., Sudarsky, D., and Hubeny, I., "Spectra and Diagnostics for the Direct Detection of Wide-Separation Extrasolar Giant Planets," *ApJ* **609**, 407–416 (July 2004).

[5] Baraffe, I., Chabrier, G., Barman, T. S., Allard, F., and Hauschildt, P. H., "Evolutionary models for cool brown dwarfs and extrasolar giant planets. The case of HD 209458," *A&A* **402**, 701–712 (May 2003).

[6] Marois, C., Macintosh, B., Barman, T., Zuckerman, B., Song, I., Patience, J., Lafreniere, D., and Doyon, R., "Direct Imaging of Multiple Planets Orbiting the Star HR 8799," *ArXiv e-prints* **322**, 1348– (Nov. 2008).

[7] Kalas, P., Graham, J. R., Chiang, E., Fitzgerald, M. P., Clampin, M., Kite, E. S., Stapelfeldt, K., Marois, C., and Krist, J., "Optical Images of an Exosolar Planet 25 Light-Years From Earth," *Science* **322**, 1–7 (Nov. 2008).

[8] Lagrange, A., Bonnefoy, M., Chauvin, G., Apai, D., Ehrenreich, D., Boccaletti, A., Gratadour, D., Rouan, D., Mouillet, D., Lacour, S., and Kasper, M., "A Giant Planet Imaged in the Disk of the Young Star β Pictoris. New deep imaging observations," *Science* (June 2010).

[9] Lafrenière, D., Jayawardhana, R., and van Kerkwijk, M. H., "Direct Imaging and Spectroscopy of a Planetary-Mass Candidate Companion to a Young Solar Analog," *ApJL* **689**, L153–L156 (Dec. 2008).

[10] Lafrenière, D., Jayawardhana, R., and van Kerkwijk, M. H., "The Directly Imaged Planet around the Young Solar Analog 1RXS J160929.1-210524: Confirmation of Common Proper Motion, Temperature and Mass," *ArXiv e-prints* (June 2010).

[11] Burrows, A., Sudarsky, D., and Lunine, J. I., "Beyond the T Dwarfs: Theoretical Spectra, Colors, and Detectability of the Coolest Brown Dwarfs," *ApJ* **596**, 587–596 (Oct. 2003).

[12] Lafrenière, D., Marois, C., Doyon, R., Nadeau, D., and Artigau, É., "A New Algorithm for Point-Spread Function Subtraction in High-Contrast Imaging: A Demonstration with Angular Differential Imaging," *ApJ* **660**, 770–780 (May 2007).

[13] Biller, B. A., Close, L. M., Masciadri, E., Nielsen, E., Lenzen, R., Brandner, W., McCarthy, D., Hartung, M., Kellner, S., Mamajek, E., Henning, T., Miller, D., Kenworthy, M., and Kulesa, C., "An Imaging Survey for Extrasolar Planets around 45 Close, Young Stars with the Simultaneous Differential Imager at the Very Large Telescope and MMT," *ApJS* **173**, 143–165 (Nov. 2007).

[14] Kasper, M., Apai, D., Janson, M., and Brandner, W., "A novel L-band imaging search for giant planets in the Tucana and β Pictoris moving groups," *A&Ap* **472**, 321–327 (Sept. 2007).

[15] Heinze, A. N., *Planets around solar-type stars: methods for detection and constraints on their distribution from an L' and M band adaptive optics imaging survey*, PhD thesis, The University of Arizona (July 2007).

[16] Racine, R., Walker, G. A. H., Nadeau, D., Doyon, R., and Marois, C., "Speckle Noise and the Detection of Faint Companions," *PASP* **111**, 587–594 (May 1999).

[17] Hinkley, S., Oppenheimer, B. R., Soummer, R., Sivaramakrishnan, A., Roberts, J. L. C., Kuhn, J., Makidon, R. B., Perrin, M. D., Lloyd, J. P., Kratter, K., and Brenner, D., "Temporal Evolution of Coronagraphic Dynamic Range and Constraints on Companions to Vega," *ApJ* **654**, 633–640 (Jan. 2007).

[18] Marois, C., Doyon, R., Racine, R., and Nadeau, D., "Efficient Speckle Noise Attenuation in Faint Companion Imaging," *PASP* **112**, 91–96 (Jan. 2000).

[19] Marois, C., Racine, R., Doyon, R., Lafrenière, D., and Nadeau, D., "Differential Imaging with a Multicolor Detector Assembly: A New Exoplanet Finder Concept," *ApJL* **615**, L61–L64 (Nov. 2004).

[20] Kenworthy, M. A., Codona, J. L., Hinz, P. M., Angel, J. R. P., Heinze, A., and Sivanandam, S., "First On-Sky High-Contrast Imaging with an Apodizing Phase Plate," *ApJ* **660**, 762–769 (May 2007).

[21] Brusa, G., Riccardi, A., Biliotti, V., del Vecchio, C., Salinari, P., Stefanini, P., Mantegazza, P., Biasi, R., Andrighettoni, M., Franchini, C., and Gallieni, D., "Adaptive secondary mirror for the 6.5-m conversion of the Multiple Mirror Telescope: first laboratory testing results," in [*Proc. SPIE Vol. 3762, p. 38-49, Adaptive Optics Systems and Technology, Robert K. Tyson; Robert Q. Fugate; Eds.*], Tyson, R. K. and Fugate, R. Q., eds., 38–49 (Sept. 1999).

[22] Lloyd-Hart, M., "Thermal Performance Enhancement of Adaptive Optics by Use of a Deformable Secondary Mirror," *PASP* **112**, 264–272 (Feb. 2000).

[23] Wildi, F. P., Brusa, G., Lloyd-Hart, M., Close, L. M., and Riccardi, A., "First light of the 6.5-m MMT adaptive optics system," in [*Astronomical Adaptive Optics Systems and Applications. Edited by Tyson, Robert K.; Lloyd-Hart, Michael. Proceedings of the SPIE, Volume 5169, pp. 17-25 (2003).*], Tyson, R. K. and Lloyd-Hart, M., eds., 17–25 (Dec. 2003).

[24] Brusa, G., Riccardi, A., Salinari, P., Wildi, F. P., Lloyd-Hart, M., Martin, H. M., Allen, R., Fisher, D., Miller, D. L., Biasi, R., Gallieni, D., and Zocchi, F., "MMT adaptive secondary: performance evaluation and field testing," in [*Adaptive Optical System Technologies II. Edited by Wizinowich, Peter L.; Bonaccini, Domenico. Proceedings of the SPIE, Volume 4839, pp. 691-702 (2003).*], Wizinowich, P. L. and Bonaccini, D., eds., *Presented at the Society of Photo-Optical Instrumentation Engineers (SPIE) Conference* **4839**, 691–702 (Feb. 2003).

[25] Freed, M., Hinz, P. M., Meyer, M. R., Milton, N. M., and Lloyd-Hart, M., "Clio: a 5-μm camera for the detection of giant exoplanets," in [*Ground-based Instrumentation for Astronomy. Edited by Alan F. M. Moorwood and Iye Masanori. Proceedings of the SPIE, Volume 5492, pp. 1561-1571 (2004).*], Moorwood, A. F. M. and Iye, M., eds., 1561–1571 (Sept. 2004).

[26] Sivanandam, S., Hinz, P. M., Heinze, A. N., Freed, M., and Breuninger, A. H., "Clio: a 3-5 micron AO planet-finding camera," in [*Ground-based and Airborne Instrumentation for Astronomy. Edited by McLean, Ian S.; Iye, Masanori. Proceedings of the SPIE, Volume 6269, pp. 62690U (2006).*], *Presented at the Society of Photo-Optical Instrumentation Engineers (SPIE) Conference* **6269** (July 2006).

[27] Guyon, O., Angel, J. R., Bowers, C., Burge, J., Burrows, A., Codona, J., Greene, T., Iye, M., Kasting, J., Martin, H., McCarthy, D. W., Meadows, V., Meyer, M., Pluzhnik, E. A., Sleep, N., Spears, T., Tamura, M., Tenerelli, D., Vanderbei, R., Woodgate, B., Woodruff, R. A., and Woolf, N. J., "Telescope to Observe Planetary Systems (TOPS): A High Efficiency Coronagraphic 1.2-m Visible Telescope," in [*American Astronomical Society Meeting Abstracts*], **209** (Dec. 2006).

[28] Codona, J. L., Hinz, P. M., Kenworthy, M. A., Angel, J. R. P., and Woolf, N. J., "High-contrast phase apodization at the MMT: design and on-sky tests," in [*Ground-based and Airborne Instrumentation for Astronomy*], McLean, I. S. and Iye, M., eds., *Proc. SPIE* **6269** (2006).

[29] Codona, J. L. and Angel, R., "Imaging Extrasolar Planets by Stellar Halo Suppression in Separately Corrected Color Bands," *ApJL* **604**, L117–L120 (Apr. 2004).

[30] Heinze, A. N., Hinz, P. M., Kenworthy, M., Miller, D., and Sivanandam, S., "Deep L'- and M-band Imaging for Planets around Vega and ϵ Eridani," *ApJ* **688**, 583–596 (Nov. 2008).

[31] Codona, J. L., Kenworthy, M. A., and Lloyd-Hart, M., "A novel WFS technique for high-contrast imaging: Phase Sorting Interferometry (PSI)," in [*Society of Photo-Optical Instrumentation Engineers (SPIE) Conference Series*], *Presented at the Society of Photo-Optical Instrumentation Engineers (SPIE) Conference* **7015** (July 2008).

[32] Codona, J., "Phase Apodization Coronagraphy," in [*In the Spirit of Bernard Lyot: The Direct Detection of Planets and Circumstellar Disks in the 21st Century*], Kalas, P., ed., 24–+ (June 2007).

[33] Riccardi, A., Brusa, G., Xompero, M., Zanotti, D., Del Vecchio, C., Salinari, P., Ranfagni, P., Gallieni, D., Biasi, R., Andrighettoni, M., Miller, S., and Mantegazza, P., "The adaptive secondary mirrors for the Large Binocular Telescope: a progress report," in [*Society of Photo-Optical Instrumentation Engineers (SPIE) Conference Series*], Bonaccini Calia, D., Ellerbroek, B. L., and Ragazzoni, R., eds., *Presented at the Society of Photo-Optical Instrumentation Engineers (SPIE) Conference* **5490**, 1564–1571 (Oct. 2004).

[34] Martin, H. M., Brusa Zappellini, G., Cuerden, B., Miller, S. M., Riccardi, A., and Smith, B. K., "Deformable secondary mirrors for the LBT adaptive optics system," in [*Society of Photo-Optical Instrumentation Engineers (SPIE) Conference Series*], *Presented at the Society of Photo-Optical Instrumentation Engineers (SPIE) Conference* **6272** (July 2006).

[35] Ida, S. and Lin, D. N. C., "Toward a Deterministic Model of Planetary Formation. II. The Formation and Retention of Gas Giant Planets around Stars with a Range of Metallicities," *ApJ* **616**, 567–572 (Nov. 2004).

[36] Kennedy, G. M. and Kenyon, S. J., "Planet Formation around Stars of Various Masses: The Snow Line and the Frequency of Giant Planets," *ApJ* **673**, 502–512 (Jan. 2008).